Stable CSR in storage rings: a model.[1]

F. Sannibale
Mail to: fsannibale@lbl.gov

J. M. Byrd, Á. Loftsdóttir, M. Venturini
Lawrence Berkeley National Laboratory, One Cyclotron Road, Berkeley, California 94720, USA

M. Abo-Bakr, J. Feikes, K. Holldack, P. Kuske, G. Wüstefeld
BESSY mbH, Albert-Einstein-Strasse 15, 12489 Berlin, Germany

H.-W. Hübers
DLR, Rutherford Strasse 2, 12489 Berlin, Germany

R. Warnock
Stanford Linear Accelerator Center, Stanford University, Stanford, California 94309, USA.

1. Introduction

A comprehensive historical view of the work done on coherent synchrotron radiation (CSR) in storage rings is given in reference [1]. Here we want just to point out that even if the issue of CSR in storage rings was already discussed over 50 years ago, it is only recently that a considerable number of observations have been reported. In fact, intense bursts of coherent synchrotron radiation with a stochastic character were measured in the terahertz frequency range, at several synchrotron light source storage rings [2-8]. It has been shown [8-11], that this bursting emission of CSR is associated with a single bunch instability, usually referred as microbunching instability (MBI), driven by the fields of the synchrotron radiation emitted by the bunch itself.

Of remarkably different characteristics was the CSR emission observed at BESSY II in Berlin, when the storage ring was tuned into a special low momentum compaction mode [12, 13]. In fact, the emitted radiation was not the quasi-random bursting observed in the other machines, but a powerful and stable flux of broadband CSR in the terahertz range. This was an important result, because it experimentally demonstrated the concrete possibility of constructing a stable broadband source with extremely high power in the terahertz region. Since the publication of the first successful experiment using the ring as a CSR source [14], BESSY II has regular scheduled user's shifts dedicated to CSR experiments. At the present time, several other laboratories are investigating the possibility of a CSR mode of operation [15-17] and a design for a new ring optimized for CSR is at an advanced stage [18].

In what follows, we describe a model that first accounts for the BESSY II observations and then indicates that the special case of BESSY II is actually quite general and typical when relativistic electron storage rings are tuned for short bunches. The model provides a scheme for predicting and optimizing the performance of ring-based CSR sources with a stable broadband photon flux in the terahertz region of up to ~ 9 orders of magnitude larger than in existing "conventional" storage rings. Such a scheme is of interest not only for the

[1] Contribution to the ICFA Beam Dynamics Newsletter No. 35

design of new sources but also for the evaluation and optimization of the CSR performance in existing electron storage rings. The presented results are mainly based on reference [19].

2. Coherent Synchrotron Radiation Basics

Coherent synchrotron radiation occurs when the electrons in a bunch emit synchrotron radiation (SR) in phase. In an intuitive picture, in a bunched beam this happens when the bunch length is comparable to the wavelength of the radiation under observation. Because of coherence, CSR intensity is proportional to the square of the number of particles per bunch in contrast to the linear dependence of the usual incoherent radiation. Since in storage rings, the number of particles per bunch is typically big (greater than ~ 10^6), the potential intensity gain for a CSR source is very large. In a more quantitative description, we have for the radiated power spectrum [20, 21]:

$$\frac{dP}{d\lambda} = \frac{dp}{d\lambda}\left[N(1-g(\lambda)) + N^2 g(\lambda)\right] \tag{1}$$

where λ is the wavelength of the radiation, p is the single particle emitted power, N is the number of particles per bunch and g is the so-called CSR form factor given by:

$$g(\lambda) = \left| \int_{-\infty}^{+\infty} n(z) e^{2\pi i \cos(\theta) z/\lambda} dz \right|^2 \tag{2}$$

where $n(z)$ is the normalized longitudinal distribution of the bunch and θ is the angle between the longitudinal direction z and the observation point. For θ equal to zero the CSR form factor is just the square of the Fourier transform of the bunch distribution. Note that, because $n(z)$ is normalized, $0 \le g \le 1$. Here $dp/d\lambda$ is defined to account for shielding due to the conductive vacuum chamber. The shielding effect has been studied by several authors over many years [22-27]. A salient feature is that $dp/d\lambda$ drops off abruptly for λ greater than the shielding cutoff wavelength λ_0, which is estimated to be about $2h\,(h/\rho)^{1/2}$, where h is the chamber total height and ρ is the radius of curvature of the particle trajectory. The first term in Eq.(1) linear in N, is the incoherent component of the power. The second term, proportional to N^2, represents the potentially much larger coherent component. Thus, to have significant CSR at the wavelength of interest we must have simultaneously $g(\lambda) > 1/(N-1) \sim 1/N$ and $\lambda < \lambda_0$. As an example, for the case of a Gaussian distribution, equation (2) can be analytically evaluated and the following criterion for the CSR emission for Gaussian bunches can be derived for $\theta = 0$:

$$\frac{2\pi\sigma_z}{\sqrt{\ln(N)}} < \lambda < \lambda_0 = 2h\left(\frac{h}{\rho}\right)^{1/2} \tag{3}$$

with σ_z the rms bunch length. Equation (3) presents a weak dependence on N variations and shows that in order to have CSR emission, we need short bunches and large cutoff wavelengths. By evaluating (3) for the case of real machines, one realizes that CSR can be practically observed in the terahertz frequency range (at 1 THz, $\lambda \sim 300$ μm). Additionally,

for most of the existing storage rings in their standard operation configuration, the bunches are usually too long and/or the vacuum chamber shielding is too strong, so that essentially no CSR can be observed. This is the reason that at BESSY II they were using a low momentum compaction lattice for shortening their bunches. But before analyzing the BESSY results, we want to do some additional consideration on the CSR form factor *g*.

3. CSR Form Factor for Non-Gaussian Longitudinal Distributions.

We are interested in investigating the CSR form factor $g(\lambda)$ for non-Gaussian bunch distributions. Figure 1, shows *g* calculated for a Gaussian distribution and for the interesting cases of two more extreme distributions: rectangular and saw-tooth like. In the example, all distributions have the same rms length.

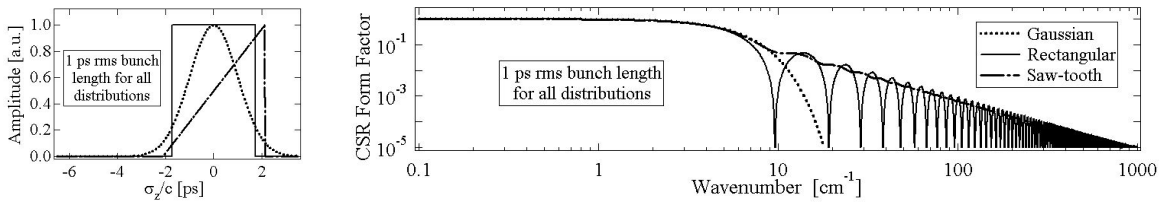

Figure 1. Gaussian, rectangular and saw-tooth like distributions and relative CSR form factors for the case of 1 ps rms bunch length. The CSR factor is expressed as a function of the wavenumber $1/\lambda$.

Figure 1 clearly shows that the two sharper edged distributions remarkably extend the CSR factor, and consequently the CSR emission, towards shorter wavelengths with respect to the Gaussian case. The saw-tooth like distribution in particular, seems to represent the "optimal" shape from the CSR point of view.

The possibility of having equilibrium distributions in storage rings approaching a saw-tooth like shape is not unrealistic. As will be better discussed in the next paragraph, several factors can generate asymmetric longitudinal distributions. For example, it is well known that any beam impedance with non-zero real part (resistive component) produces asymmetric bunches with a sharper edge.

The bunch distribution in the BESSY II low momentum compaction configuration used for the CSR production, was significantly asymmetric, as proved by streak camera measurements [28] and by the fact that the extension of the high frequency part of the measured CSR spectra in [13] cannot be explained by assuming Gaussian bunches.

4. Generating Non-Gaussian Bunches.

Low current equilibrium longitudinal distributions in electron storage rings are usually Gaussian. Anyway, several factors can contribute to "distort" the bunch distribution. In order to understand the BESSY II results and to eventually find a way to generate saw-tooth like distributions in a storage ring, we need to consider all such factors and evaluate their relative importance. We can classify them into two main categories: nonlinear dynamics and collective effects. Radio frequency (RF) and lattice nonlinearities belong to the first group, while SR and conductive vacuum chamber wakefields fall into the second one.

4.1 Nonlinear Dynamics Effects.

For most storage rings RF nonlinearities are very small and can be neglected. The situation can be different when the storage ring includes a higher harmonic RF system. Such

systems are specifically designed to modify the bunch distribution and their effect must be accounted for. At BESSY II, there is a higher harmonic system but it is passive and at the very low currents of the CSR mode of operation (few tens of μA/bunch) its effect is negligible.

We want now to investigate the case of strong lattice nonlinearities. As explained earlier, short bunches are preferred for producing CSR and a typical way to shorten the bunch is by lowering the storage ring momentum compaction. Anyway, for very small momentum compaction values (smaller than ~10^{-5}), as the ones used in the BESSY II CSR lattice, the energy dependent terms of the momentum compaction can become important and generate strong distortions of the orbits in the longitudinal phase space. Such a situation can potentially lead to non-Gaussian equilibrium distributions. We have done extensive simulations using the BESSY II parameters and also investigating the case of extremely distorted longitudinal phase space topologies. The clear result was that lattice nonlinearities can generate significant distortions in the energy distribution of the bunch but very small distortions of the spatial distribution.

4.2 Collective Effects.

In the analysis of the collective effects we start first with the wakes due to the SR in a bending magnet, and later consider the ones associated with the vacuum chamber. A large number of storage rings have insertion devices (ID) but in our analysis we will not consider their SR wakes. In a ring with IDs, this is the equivalent of assuming that the ID gaps are open (as they were during the BESSY II CSR measurements). Analytical expressions for the SR radiation wake in a wiggler have been derived [29] and could be used for further investigation.

For the SR wake in the bends, we use the analytical expressions where the vacuum chamber shielding is represented by the parallel plates model [22-27]. In "standard" wakes, the fields excited in the vacuum chamber by the particles in the head of the bunch can only affect the particles in the tail. In the SR radiation wake case, it is exactly the opposite, the particles in the tail modify the energy of the ones in the head. This happens when a relativistic electron in a bunch is traveling on a curved trajectory radiating SR. Contrarily to the electron, the emitted photons proceed on a straight line and because of this, the electron velocity component parallel to the photon trajectory is smaller than the photon speed. This allows for a photon emitted in the tail of the bunch to reach the electrons in the head and to interact with them.

To find the equilibrium longitudinal bunch distribution in the presence of wakes we use the well known Haïssinski equation [30]:

$$I(\tau) = K \exp\left[-\frac{(c\tau)^2}{2\sigma_{zo}^2} - \frac{c^2}{\sigma_{zo}^2 \dot{V}_{RF}} \int_{-\infty}^{\infty} I(\tau - t) S(t) dt \right] \tag{4}$$

where $I(\tau)$ is the longitudinal current distribution, τ is position of the particle in the bunch in time units, c is the speed of light, σ_{zo} is the natural bunch length, $\dot{V}_{RF}$ is the time derivative of the radio frequency voltage at the synchronous phase, K is a normalization constant and $S(t)$ is the wake in the step response form:

$$S(t) = \frac{2\pi\rho}{e} \int_{-\infty}^{t} E_w(t')dt' \tag{5}$$

with e the electron charge and E_w the electric field associated to the wake under consideration. The integration limits in Eq. (4) and Eq. (5) are for the general case of wakes with nonzero values in front and behind the generating particle (combination of vacuum chamber and SR wakes).

Figure 2 shows the numerical solutions of equation (4) for the case of BESSY II for different currents per bunch and using the shielded SR wake. The results show several interesting features: with growing current per bunch, the distribution leans forward with an increasingly sharp leading edge, the bunch rear becomes less steep, the bunch centroid shifts to earlier times (synchronous phase shift) and the rms length of the distribution increases but only slightly. It is worth noticing that the calculated distributions clearly lean towards the CSR ideal saw-tooth like shape. The "hump" on the highest current curve is due to the shielding effect of the vacuum chamber.

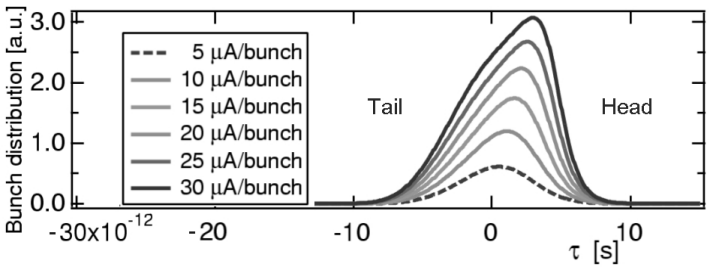

Figure 2. Calculated equilibrium distributions using the shielded SR wake. Case of the BESSY II in the configuration for CSR production.

For a quantitative comparison with the BESSY results, we define for a given current and wavenumber ($1/\lambda$), the CSR gain as the ratio between the radiation intensities when CSR is present and when the emission is completely incoherent. This new quantity has the big advantage with respect to the absolute flux, that it is independent of the calibration of the measurement system. Its value approaches 1 when the CSR emission is very small ($g \sim 0$) and N when it is large ($g \sim 1$). Figure 3 shows the CSR gain measured at BESSY II [13] and the calculated distributions as a function of the radiation wavenumber for two different currents per bunch. Also shown is the calculated CSR gain for the undistorted Gaussian distribution. The shaded areas represent the shielded SR calculations obtained by varying the natural bunch length over a 10% range. This choice can be explained as follows. The natural bunch length used as input parameter for the simulations was derived from measurements of the synchrotron frequency, of the RF voltage and of other machine quantities. The experimental error for this evaluation is consistent with a 10% uncertainty.

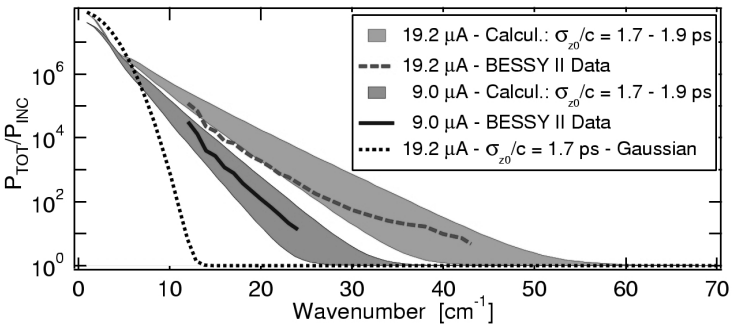

Figure 3. CSR gain as a function of the wavenumber. The BESSY II data for two different currents per bunch are compared with the shielded SR calculation and with the curve for a Gaussian distribution of the same length.

The comparison in Fig.3 shows the general good agreement between calculations and data and also the strong power enhancement at the higher wavenumbers that the distorted case presents with respect to the Gaussian one. In Ref. [13] a 40 μA curve is also shown, but the data are unusable for comparison because of the presence of CSR bursting, this current being above MBI threshold [8-11].

We will now introduce in our analysis the vacuum chamber wakes starting with the resistive wall (RW) one [31, 32]. The nonzero resistivity of the storage ring vacuum chamber is responsible for this wake that, when strong enough, can produces equilibrium bunch distributions with the saw-tooth like shape similar to the SR wake case. In our calculations, the long range approximation for the RW wake was used, being appropriate for the BESSY II case. Figure 4 shows, for a particular case of BESSY II, the comparison between the CSR gain curves calculated using the shielded SR wake with (dotted line) and without (dashed line) the inclusion of the RW wake. The effect of the RW wake is clearly very small and slightly decreases the CSR gain.

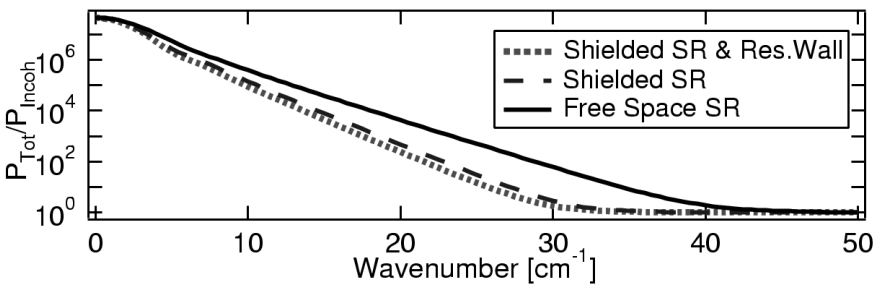

Figure 4. CSR gain vs. radiation wavenumber calculated using the shielded SR wake with (dotted line) and without (dashed line) the resistive wall wake. The solid line shows the gain calculated with the free space SR wake. Case of BESSY II with 9.0 μA per bunch and 1.7 ps natural bunch length.

.

It is somehow surprising that the RW wake decreases the CSR gain. In fact, by producing the same kind of distortion of the SR wake, one would expect an increase in the CSR gain. The explanation is that the RW generates at the same time a significant bunch lengthening, which reduces the CSR emission at shorter wavelengths. This second effect is stronger than the distortion enhancement and the net result is a decrease of the CSR gain.

Additional calculations using different models for the BESSY II vacuum chamber broadband impedance showed a negligible contribution from this kind of wake at these low current-short bunches conditions.

5. The Free Space SR Wake Regime.

The solid line in Fig .4 shows the CSR gain calculated using the free space (FS) SR wake [25, 26] for the interesting case where the vacuum chamber shielding is negligible. Compared to the FS case, the vacuum chamber shielding reduces the gain significantly, pointing out the important result that for maximizing the CSR gain in an optimized source the shielding effect must be kept negligible.

For the case of the parallel plates model and Gaussian bunches, a simple criterion for the shielding importance is given by [25]:

$$\Sigma = \frac{\sigma_z}{h}\left(\frac{2\rho}{h}\right)^{1/2} \leq 0.2 \tag{6}$$

If Eq. (6) is fulfilled, then the shielding effect is negligible and the FS SR wake can be used (note that $\Sigma \propto \sigma_z/\lambda_0$). Two examples: in the case of BESSY II with $\sigma_z \sim 1$ mm, $\rho = 4.35$ m and $h = 3.5$ cm, $\Sigma \sim 0.45$ and the shielding effect is relevant, while in a hypothetical but realistic CSR source with $\sigma_z = 300$ μm, $h = 4$ cm and $\rho = 1.33$ m, $\Sigma \sim 0.06$ and the shielding is negligible.

Summarizing, we have seen that it is possible to design a realistic storage ring where the shielding effects are negligible. Additionally, by using for the vacuum chamber a low resistivity material, aluminum for example, we will be able to control the effects of the RW wake down to negligible levels as well. We also showed that in this situation, the FS SR wake becomes dominant and the CSR emission is maximized.

We need now to understand how to exploit this situation for the optimization of a CSR source quantitatively. The FS SR wake, in the step response shape, can be expressed with very good approximation as [25-27]:

$$S(\tau) \cong \begin{cases} -Z_0\left(\dfrac{\rho}{3c}\right)^{1/3}\tau^{-1/3} & \tau > 0 \\ 0 & \tau \leq 0 \end{cases} \tag{7}$$

with $Z_0 = \mu_0 c = 376.7\ \Omega$. Figure 5 shows an example of equilibrium bunch distributions obtained by solving the Haïssinski equation using the wake (7) for positive momentum compaction. Again, as in the shielded case of Fig. 2, the asymmetry increases with current but now, at the higher currents, the hump is disappeared and the curves are really close to the ideal saw-tooth like shape.

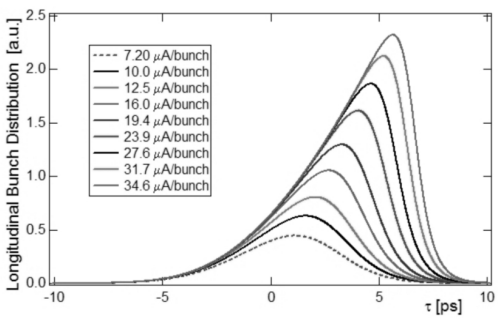

Figure 5. Example of calculated bunch distributions for the case of the free space SR wake and positive momentum compaction.

Based on this result, one could think that for maximizing the CSR emission, it is sufficient to keep increasing the current per bunch. Unfortunately, there is a limit and this is set by the MBI, the same instability responsible for the CSR burst mentioned in the introduction.

6. The Microbunching Instability.

We discuss now the case of the MBI that can be excited by the SR radiation wake in the bends of electron storage rings [8-11]. Fluctuations in the longitudinal bunch

distribution, with characteristic length shorter than the bunch length, can radiate coherently. Above a current per bunch threshold, the SR emission becomes strong enough to enhance these longitudinal fluctuations, triggering a chain effect leading to microbunching and instability. The appearance of such microstructures is associated with the emission of burst of CSR in the terahertz frequency range. Indicating with N_{MBI} the threshold, a stability criterion for the MBI can be expressed as [8-10]:

$$N \le N_{MBI} = A\left(\frac{B}{E}\right)^{1/3} f_{RF} V_{RF} \frac{\sigma_{z0}^3}{\lambda^{2/3}} \tag{8}$$

with $A = \left(2^{1/2}\pi^{7/6} e^{4/3} / r_0 m_0 c^{8/3}\right) = 4.528 \times 10^{-3}$ [SI units], r_0 the electron classical radius, m_0 its rest mass, B the magnetic field in the bend magnet, f_{RF} and V_{RF} the frequency and the peak voltage of the RF system respectively and E the beam energy.

For the large majority of the experiments using terahertz radiation, stability of the photon flux is a fundamental requirement. In a storage ring, the MBI with its terahertz bursts can seriously jeopardize the performance as a CSR source if not controlled.

In the next paragraph, we describe a scheme that allows to adjust the parameters of a ring such that the CSR power and bandwidth are maximized while remaining below the threshold for the MBI.

7. On Optimized Stable CSR Source Based on a Storage Ring.

Assuming that criterion (6) is fulfilled and that all the other wakes are negligible, we can use the FS SR wake and following the approach used in ref. [33] we express the bunch population N as:

$$N = \frac{1}{ec^2 Z_0}\left(\frac{3}{\rho}\right)^{1/3} \dot{V}_{RF}\, \sigma_{z0}^{7/3} F(\kappa) \tag{9}$$

The numerical factor $F(\kappa) = \int_{-\infty}^{\infty} y_\kappa(x)\, dx$ is the integral of the solution of the equilibrium equation:

$$y_\kappa(x) = \kappa \exp\left[-\frac{x^2}{2} + \mathrm{sgn}(\alpha)\int_0^{\infty} y_\kappa(x-z) z^{-1/3} dz\right] \tag{10}$$

which is a dimensionless form of the Haïssinski equation (4) for the special case of the FS SR wake (7), with $x = c\tau/\sigma_{z0}$ and $y_\kappa = \left(Z_0 c/\dot{V}_{RF}\right)\left(\rho/3\sigma_{z0}^4\right)^{1/3} I$. The factor sgn ($\alpha$) is the sign of the momentum compaction α. The quantity F depends only on the dimensionless normalization parameter κ. As κ increases, F, N, and the bunch distortion all increase. F can be thought as a quantitative indication of the bunch distortion: the larger F the larger the distortion and, for what we have shown in the previous paragraphs, the more extended is the CSR spectrum.

For a linear RF system at the synchronous phase, $\dot{V}_{RF} = 2\pi f_{RF} V_{RF}$ and for a relativistic electron storage ring, $\rho = E/ecB$, which used in (9) give:

$$N = C\left(\frac{B}{E}\right)^{1/3} f_{RF} V_{RF} \sigma_{z0}^{7/3} F(\kappa) \tag{11}$$

with $C = (2\pi/Z_0)\left(3/e^2c^5\right)^{1/3} = 6.068\times10^{-4}$ [SI units].

The expression for $dp/d\lambda$ when the wavelength is shorter than λ_0 but much larger than the SR critical wavelength, is given by [31]:

$$\frac{dp}{d\lambda} = \left(\frac{2^{10}\pi^7 c^8}{3e}\right)^{1/3} \frac{r_0 m_0}{\Gamma(1/3)} \frac{1}{L}\left(\frac{E}{B}\right)^{1/3} \frac{1}{\lambda^{7/3}} \tag{12}$$

with L the ring length and with the gamma function $\Gamma(1/3) \sim 2.679$, By using Eq. (11), Eq. (12) in Eq. (1) for $Ng(\lambda) >> 1$, we can write the power spectrum for a ring with N_b bunches as:

$$\frac{dP}{d\lambda} = D\frac{N_b}{L}(f_{RF}V_{RF})^2\left(\frac{B}{E}\right)^{1/3}\left(\frac{\sigma_{z0}^2}{\lambda}\right)^{7/3} F(\kappa)^2 g(\lambda) \tag{13}$$

with $D = \left(2^{16}\, 3\, \pi^{13}/e^5c^2\right)^{1/3}\left(r_0 m_0/Z_0^2\Gamma(1/3)\right) = 2.642\times10^{-21}$ [SI units].

To optimize the intensity and spectral bandwidth given by (13) we must first be sure that our distribution is stable. Or in other words, that the bunch population is maintained below the threshold for the MBI. By combining Eq. (8) and Eq. (11), the following stability criterion is obtained:

$$F \le F_{\max} = G(\sigma_{z0}/\lambda)^{2/3} \tag{14}$$

where $G = \left(2^{3/2}\pi^{7/6}/3^{1/3}\right) \cong 7.456$ is a dimensionless constant. It must be remarked that the MBI theory was derived for the case of a coasting beam. Anyway, simulations and experimental results at the Advanced Light Source (ALS) in Berkeley and at BESSY II [10, 11] showed that the model works also for bunched beams and that the theory is able to predict the instability threshold when in Eq. (8) $\lambda \sim \sigma_{z0}$. By (14) the corresponding threshold for F becomes:

$$F \le F_{\max} \approx G \tag{15}$$

The value of κ for maximum F is obtained by solving (10), increasing κ to a value κ_{max} (~ 0.292, for the positive momentum compaction case) such that $F(\kappa_{max}) = G$.

Now let us examine the terms of Eq. (13) with more attention. Expressing the CSR form factor g (Eq. (2)) in terms of y_κ, we find for $\theta = 0$:

$$g(\lambda)=\frac{1}{F(\kappa)^2}\left|\int_{-\infty}^{\infty} y_\kappa(x)\, e^{i2\pi\frac{\sigma_{z0}}{\lambda}x}\, dx\right|^2 \tag{16}$$

Eq. (16) shows that, in the case of the FS SR wake, $g(\lambda)$ is a function only of the ratio σ_{z0}/λ and of κ. It is interesting to notice that for large λ values, the integral in Eq. (16) tends to F so that g tends to 1. Figure 6 shows $y_{\kappa max}(x)$ and Eq. (16) for positive momentum compaction and for the CSR optimized case when $\kappa = \kappa_{max}$.

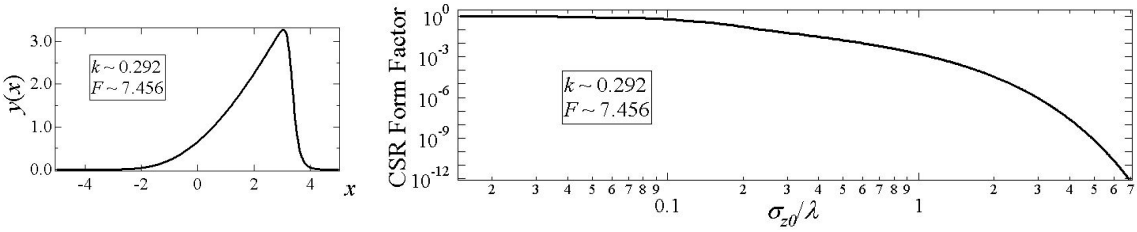

Figure 6. The "universal" distribution $y_{\kappa max}$ and CSR form factor for the case of the FS SR wake, calculated for $\kappa = \kappa_{max}$ and positive momentum compaction.

The curve in the right part of Fig.6 allows to calculate the CSR form factor of the optimized source, by knowing only the natural bunch length σ_{z0}, while the curve on the left defines the bunch distribution when σ_{z0} and N are known. N is simply given by (11) with F replaced by G. The CSR spectrum for our stable optimized source is now completely defined and can be evaluated by using Eq. (1).

We want now to choose our parameters in order to maximize the CSR bandwidth and power. Eq. (16) shows that, for a fixed κ (κ_{max} in our case), the spectrum extends to larger wave numbers as σ_{z0} is decreased. On the other hand, the factor $\sigma_{z0}^{14/3}$ in Eq. (13) sharply degrades the overall intensity if σ_{z0} is too small. By an appropriate compromise in the choice of σ_{z0} we get a suitable spectral bandwidth.

Once that choice is made and we have set $F = G$ in Eq. (13), we can still vary the other factors in this equation to maximize radiation intensity while respecting technical constraints. Explicitly, Eq. (13) asks for i) a large peak RF voltage V_{RF}, this can be obtained by superconductive systems but of course with increased costs; ii) a high bending magnet magnetic field B, but the same arguments used for V_{RF} apply also here; iii) a high f_{RF}, but for example, availability of high frequency systems, coupled bunches instabilities and cavities aperture could become an issue; iv) a lower beam energy E, but the decreased stiffness and the weaker damping could represent a problem from the accelerator physics point of view; v) a small L, which will make the ring more compact and less expensive, but on the other hand a longer ring serves more users and the presence of reasonably long straight sections can allow for insertion devices and for several possible interesting applications and upgrades [18].

It must be remarked that the momentum compaction, which does not appear explicitly in Eq. (13), is used in this scheme for keeping constant σ_{z0} when the other quantities are varied.

Figure 7 shows an example of the impressive performance that a source designed with the presented criteria can achieve. In this particular combination of the Eq. (13) parameters,

three modes of operation, trading between power and bandwidth, are plotted and can be selected with continuity by simply tuning the lattice momentum compaction from 4.3×10^{-4} to 3.9×10^{-3}. Also shown for comparison are the curves for a "conventional" SR source (the ALS) and for BESSY II in the special CSR mode.

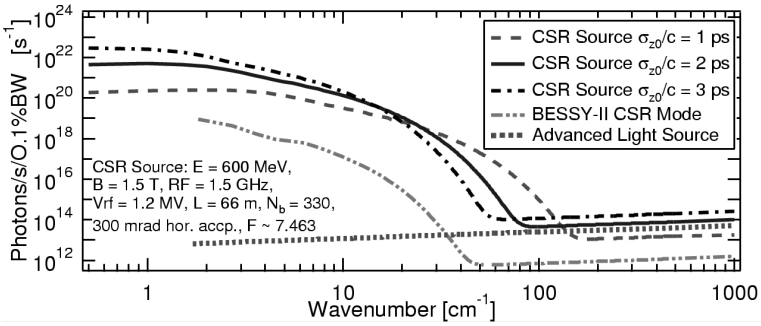

Figure 7. Example of source optimized for the CSR production using the criteria described in this paper. The photon flux is compared with the cases of a conventional SR source (ALS) and of BESSY II CSR mode with 400 bunches, 19.2 μA/bunch, σ_{z0}/c = 1.8 ps and 60 mrad horizontal acceptance..

Criterion (15), when used in Eq.(11) with a given σ_{z0}, sets the threshold for the single bunch current that can be stored without experiencing the MBI. The strong dependence of this threshold on σ_{z0} explains why the SR wake becomes dominant in the short bunch regime, making the longitudinal dynamics practically independent from the vacuum chamber wakes. This result has the quite general implication that very short and stable bunches can be obtained only at the cost of very small currents per bunch. For example, in our hypothetical CSR source of Fig. 7, in order to go from σ_{z0} equal to 3 ps to 1 ps, the current per bunch must drop from ~ 1.2 mA to ~ 90 μA to preserve stability.

We have analyzed only the case for positive momentum compaction. For negative values of this parameter, the situation is similar but not completely identical. For example, as shown in [33], a comparable saw-tooth distortion of the distribution is obtained but also some simultaneous bunch lengthening. This does not seem to be promising from the CSR point of view but for an accurate answer a complete analysis is necessary.

Eq. (9) shows that N is proportional to the time derivative of the RF voltage. For simplicity, in our analysis we have assumed a single RF system with frequency f_{RF}. In the more general case, we could have the simultaneous presence of different systems with different frequencies. In particular, as suggested in [35], it could be interesting to study the case where an additional higher harmonic RF system is used for increasing the absolute value of the RF voltage derivative at the synchronous phase.

8. Conclusions.

We have presented a model that describes CSR in electron storage rings. We used it for explaining the observations at BESSY II and for developing ring based sources optimized for the CSR generation in the terahertz frequency range, with photon flux up to 9 orders of magnitude larger than in existing conventional storage rings. In particular, it has been shown that the CSR performance is maximized when the vacuum chamber shielding is negligible and the synchrotron radiation wake dominates over the vacuum chamber ones. Stability criteria for controlling the synchrotron radiation induced microbunching instability were included as well, in order to generate a stable flux of CSR as required from most

terahertz applications. The model can be also used for predicting the CSR possibilities for existing storage rings.

A quite general result of our analysis is that for storage rings in the short bunches regime (~ 1 ps), the synchrotron radiation wake becomes dominant determining alone the longitudinal dynamics of the bunch. In this situation, the intensity of the wake becomes so intense that the induced microbunching instability severely limits the maximum stable current per bunch to very low values.

Finally, we want to remark that the CSR enhancement at shorter wavelengths due to SR induced bunch distortions was first mentioned in Ref. [33].

9. Acknowledgements.

We acknowledge contributions of M. C. Martin, D. Robin, E. Forest, J. Murphy, and U. Schade. This work was supported by the Director, Office of Science, U.S. Department of Energy under Contracts No. DE-AC03-76SF00098 and No. DE-AC03-76SF00515.

10. References.

[1] J. B. Murphy, this newsletter.
[2] A.R. Hight-Walker, *et al.*, Proc. SPIE Int. Soc. Opt. Eng. **3153**, 42 (1997).
[3] M. Berger, Nucl. Instrum. Methods Phys. Res. Sect. A **395**, 259 (1997).
[4] G. L. Carr, *et al.*, Proceeding of the 1999 IEEE Particle Accelerator Conference, New York, NY, March 1999, p. 134, and Nucl. Instrum. Methods Phys. Res. Sect. A **463**, 387 (2001).
[5] Å, Anderson, *et al.*, Opt. Eng. (Bellingham, Wash.) **39**, 3099 (2000).
[6] M. Abo-Bakr, *et al.*, Proceedings of the 7th European Particle Accelerator Conference, Vienna, 2000, p. 720.
[7] U. Arp, *et al.*, Phys. Rev. ST Accel. Beams **4**, 054401 (2001).
[8] J. M. Byrd, *et al.*, Phys. Rev. Lett. **89**, 224801 (2002).
[9] S. Heifets and G. Stupakov, Phys. Rev. ST Accel. Beams **5**, 054402 (2002).
[10] M. Venturini and R. Warnock, Phys. Rev. Lett. **89**, 224802 (2002).
[11] M. Abo-Bakr, *et al.*, Proceeding of the 2003 IEEE Particle Accelerator Conference, Portland, OR, 2003, p. 3023.
[12] M. Abo-Bakr, *et al.*, Phys. Rev. Lett. **88**, 254801 (2002).
[13] M. Abo-Bakr, *et al.*,, Phys. Rev. Lett. **90**, 094801 (2003).
[14] J. Singley, *et al.*, Phys. Rev. B. **69**, 092512 (2004).
[15] C. Biscari, *et al*., DAΦNE Technical Note G-61, July 28, 2004.
[16] The Metrology Light Source of the Physikalisch-Technische Bundesanstalt under construction in Berlin-Adlershof (Germany).
[17] ESRF, Grenoble, France, this newsletter.
[18] J. M. Byrd, *et al.*, Proceedings of the 9th European Particle Accelerator Conference, Lucerne, 2004, p. 2433.
[19] F. Sannibale, *et al.*, Phys. Rev. Lett. **93**, 094801 (2004).
[20] L.I. Shift, Rev. Sci. Instr. **17**, 6 (1946).
[21] G. Williams, *et al.*, Phys. Rev. Lett. **62**, 261 (1989).
[22] J. Schwinger, Phys. Rev. **70**, 798 (1946) and LBNL-39088 (1966).
[23] J. S. Nodvick and D. S. Saxon, Phys. Rev. **96**, 180 (1954)
[24] R. Warnock and P. Morton, Part. Accel. **25**, 113 (1990).

[25] J. B. Murphy, S. Krinsky and R. L. Gluckstern, Proceeding of the 1995 IEEE Particle Accelerator Conference, Dallas, TX, May 1995, p. 2980 and Part. Accel. **57**, 9 (1997).
[26] Y. S. Derbenev, *et al.*, DESY Report No. TESLA-FEL 95-05, 1995.
[27] G. Stupakov and I. Kotelnikov, Phys. Rev. ST Accel. Beams **6**, 034401 (2003).
[28] M. Abo-Bakr, *et al.*, Proceeding of the 2003 IEEE Particle Accelerator Conference, Portland, OR, 2003, p. 3020.
[29] J. Wu, *et al.*, Phys. Rev. ST Accel. Beams **6**, 040701 (2003).
[30] J. Haïssinski, Il Nuovo Cimento **18B**, 72 (1973).
[31] A. W. Chao, *Physics of Collective Beam Instabilities in High Energy Accelerators* (Wiley, New York, 1993).
[32] K. Bane and M. Sands, in *Micro-Bunches Workshop, Upton, NY, 1995*, edited by E. B. Blum *et al.*, AIP Conf. Proc. No. 367 (AIP, New York, 1996), p. 131.
[33] K. Bane, S. Krinsky, and J. B. Murphy, in *Micro-Bunches Workshop, Upton, NY, 1995*, edited by E. B. Blum *et al.*, AIP Conf. Proc. No. 367 (AIP, New York, 1996), p.191.
[34] A. Hofmann, in *" Synchrotron Radiation and Free Electron Lasers"*, CERN Report No. CAS-CERN-98-04, 1998, p. 1.
[35] J. Feikes, *et al.*, Proceedings of the 9th European Particle Accelerator Conference, Lucerne, 2004, p. 1951.